# Supplementary Material S1: Data

## *In vivo tumor growth studies in PDX mice*

*Table S1.1 – Considered PDX mouse models*.

| BR | CC | CR | GA | HN | LI | LU ADC | LU SCC | ME | PA | SA |
|---|---|---|---|---|---|---|---|---|---|---|
| BR10014 | CC6679 | CR0004 | GA0006 | HN0366 | LI0050 | LU1147 | LU0350 | ME1154 | PA0372 | SA0639 |
| BR10539 | CC6639 | CR0012 | GA0023 | HN0586 | LI0348 | LU11606 | LU0357 | ME11971 | PA0692 | SA10199 |
| BR10582 | CC6638 | CR0150 | GA0044 | HN0696 | LI0612 | LU1235 | LU0367 | ME11972 | PA1194 | SA13127 |
| BR1115 | CC6279 | CR0170 | GA0046 | HN1972 | LI0801 | LU1380 | LU0395 | ME12035 | PA1198 | SA13226 |
| BR1282 | CC6216 | CR0193 | GA0055 | HN2174 | LI1005 | LU1452 | LU0697 | ME12047 | PA1222 | SA13389 |
| BR1283 | CC0449 | CR0196 | GA0080 | HN2221 | LI1025 | LU2038 | LU0741 | ME12056 | PA1233 | SA3224 |
| BR1458 | CC11307 | CR0205 | GA0087 | HN2574 | LI1035 | LU2049 | LU0743 | ME12057 | PA1265 | SA3283 |
| BR1474 | CC1470 | CR1519 | GA0095 | HN2576 | LI1037 | LU2071 | LU0884 | ME12068 | PA1280 | SA3296 |
| BR2014 | CC6204 | CR1801 | GA0098 | HN2581 | LI1054 | LU2505 | LU1143 | ME12070 | PA1301 | SA3829 |
| BR3267 | CC6205 | CR2110 | GA0119 | HN2583 | LI1055 | LU2535 | LU1155 | ME12079 | PA1306 | SA3831 |
| BR5009 | CC6600 | CR2161 | GA0138 | HN2586 | LI1058 | LU5165 | LU1160 | ME12080 | PA1332 | SA4062 |
| BR5010 | CC6604 | CR2394 | GA0151 | HN2594 | LI1069 | LU5176 | LU1204 | ME12107 | PA1338 | SA4094 |
| BR5011 | CC6607 | CR2517 | GA0318 | HN2606 | LI1074 | LU5187 | LU1206 | ME12120 | PA1390 | SA4097 |
| BR5013 | CC6609 | CR2518 | GA0429 | HN3504 | LI1078 | LU5194 | LU1423 | ME12149 | PA2410 | SA4109 |
| BR5015 | CC6614 | CR2519 | GA2101 | HN3508 | LI1081 | LU5209 | LU1661 | ME12172 | PA3013 | SA4128 |
| BR6695 | CC6625 | CR2524 | GA2278 | HN3537 | LI1097 | LU5212 | LU1690 | ME12208 | PA3029 | SA4148 |
| BR9456 | CC6637 | CR2814 | GA3055 | HN3642 | LI1098 | LU5240 | LU1776 | ME12212 | PA3065 | |
| BR9464 | CC6645 | CR3079 | GA3121 | HN3674 | LI6206 | LU5245 | LU3075 | ME12216 | PA3126 | |
| BR9465 | CC6658 | CR3150 | GA3158 | HN3690 | LI6280 | LU5247 | LU6439 | ME12217 | PA3127 | |
| BR9466 | CC6680 | CR3315 | GA3839 | HN3712 | LI6281 | LU5349 | LU6440 | ME12222 | PA3136 | |
| BR9469 | CC6724 | CR3496 | GA6200 | HN3792 | LI6605 | LU5371 | LU6901 | ME13996 | PA3137 | |
| BR9479 | CC9326 | CR3612 | GA6212 | HN3796 | LI6610 | LU5381 | LU6905 | ME2194 | PA3139 | |
| BR9480 | CC9506 | CR6219 | GA6822 | HN5111 | LI6611 | LU6412 | LU6917 | ME2319 | PA6233 | |
| BR9493 | | CR6227 | GA6877 | HN5125 | LI6612 | LU6414 | LU9357 | ME5285 | PA6259 | |

**PDX codes from HuBase database (Crownbio Bioscience Inc., https://www.crownbio.com/).*

## *Curation of TVDT data in untreated cancer patients*

Twenty-six studies reporting the values of TVDT in untreated cancer patients were retrieved from the literature. Table S1.2 lists the reported median, minimum and maximum TVDT and the population size for each study.

Clinical data showed that the frequency distribution of TVDT obtained using the Schwartz's formula (Eq.1) is positively skewed, with some very long TVDTs compared with the typical value **(5)**. Therefore, to reduce the impact of these outliers, a range of TVDT variation was estimated for each of the considered studies based on the following strategy. For each study:

- TVDT was supposed to be log-normally distributed **(15,44)**, i.e., $\boldsymbol{TVDT = TVDT_{median}\exp(\eta)}$ with $\boldsymbol{\eta \sim \mathcal{N}(0,\sigma^2)}$ and $\boldsymbol{TVDT_{median}}$ fixed to the reported median;
- the observed $[\boldsymbol{TVDT_{minimum}}, \boldsymbol{TVDT_{maximum}}]$ range was supposed representative of the 95%CI of TVDT; consequently, the 95%CI of $\boldsymbol{\eta}$ was given by $\left[\ln\left(\frac{TVDT_{minimum}}{TVDT_{median}}\right), \ln\left(\frac{TVDT_{maximum}}{TVDT_{median}}\right)\right] = [-2\sigma, 2\sigma]$, as $\boldsymbol{\eta}$ is normally distributed with zero mean; thus, $\boldsymbol{\sigma}$ could be approximated as $\boldsymbol{\sigma = \ln\left(\frac{TVDT_{maximum}}{TVDT_{minimum}}\right)/4}$;
- 10th and 90th percentiles (*p10* and *p90*) of $\boldsymbol{\eta}$ were computed;
- the range of TVDT (80% CI) was approximated with $[\boldsymbol{TVDT_{median}e^{p10}}, \boldsymbol{TVDT_{median}e^{p90}}]$.

For cancer type for which multiple studies are available, the geometric means of the medians weighted by the corresponding number of patients, $\overline{\boldsymbol{TVDT_{median}}}$, were used to summarize the typical TVDT value. In addition, a unique log-normal distribution was reconstructed for each cancer type and parametrized as $\boldsymbol{TVDT =}$

$\overline{TVDT_{median}}\,\mathbf{exp}(\boldsymbol{\varphi})$ with $\boldsymbol{\varphi} \sim \boldsymbol{\mathcal{N}}(\mathbf{0}, \boldsymbol{\omega}^{\mathbf{2}})$ where the variance $\boldsymbol{\omega}^{\mathbf{2}}$ was computed as the algebraic mean of the $\boldsymbol{\sigma}^{\mathbf{2}}$ weighted by the number of patients. From the obtained distributions, a unique range, 80% CI, for each cancer type was derived considering $[\overline{TVDT_{median}}e^{p10}, \overline{TVDT_{median}}e^{p90}]$.
The predicted TVDT ranges stratified by study and cancer type were reported in Table S2.1.

*Table S1.2 Observed TVDT [month] in untreated cancer patients stratified by study and cancer type.*

| Cancer Type | Reference | N. pz | Individual TDVT data | Median TVDT [month] | Reported TVDT range [month] | Estimated 80%CI of TVDT [month] | Estimated median TVDT for cancer type [month] | Estimated sd*, $\omega_{TVDT}$, for cancer type [-] | Estimated 80%CI of TVDT by cancer type [month] |
|---|---|---|---|---|---|---|---|---|---|
| BR | Fournier **(19)** | 147 | Y | 7.97 | [1.47, 62.3] | [2.4, 26.7] | 5.66 | 0.84 | [1.92, 16.55] |
| | Gershon-Cohen **(20)** | 18 | Y | 4 | [0.77, 6.97] | [1.98, 8.12] | | | |
| | Ryu **(21)** | 66 | N | 4.7 | [1.53, 27.5] | [1.87, 11.85] | | | |
| | Tabbane **(22)** | 75 | N | 3.83 | [0.47, 25.73] | [1.06, 13.76] | | | |
| | Zhang **(23)** | 69 | N | 5.47 | [2.2, 17.37] | [2.81, 10.66] | | | |
| CC | De Rose **(24)** | 79 | N | 2.33 | [0.48, 17.07] | [0.75, 7.32] | - | 0.89 | - |
| CR | Bolin **(25)** | 27 | N | 4.33 | [1.77, 52.33] | [1.46, 12.93] | 6.12 | 0.59 | [2.87, 13.02] |
| | Burke **(26)** | 43 | N | 7.03 | [3.73, 13.47] | [4.66, 10.59] | | | |
| | Tada **(27)** | 12 | Y | 8.11 | [3.08, 34.41] | [3.75, 17.44] | | | |
| GA | Haruma **(28)** | 12 | Y | 8.1 | [2.2, 23.4] | [3.8, 17.22] | 8.57 | 0.74 | [3.33, 22.16] |
| | Seung-Young **(29)** | 97 | N | 8.63 | [1, 21.1] | [3.27, 22.97] | | | |
| HN | Jensen **(30)** | 61 | N | 3.3 | [0.5, 7.8] | [1.36, 7.96] | 2.99 | 0.68 | [1.26, 7.18] |
| | Waaijer **(31)** | 13 | Y | 1.9 | [0.7, 8.53] | [0.85, 4.25] | | | |
| LI | Barbara **(32)** | 58 | N | 5.72 | [0.91, 20.19] | [2.12, 15.28] | 3.22 | 0.68 | [1.35, 7.7] |
| | Kubota **(33)** | 22 | N | 2.77 | [1.08, 16.55] | [1.16, 6.63] | | | |
| | Park **(34)** | 59 | Y | 2.03 | [0.7, 6.97] | [0.98, 4.22] | | | |
| | Sheu **(35)** | 30 | Y | 3.9 | [0.97, 13.27] | [1.69, 8.96] | | | |
| | Nakajima **(36)** | 34 | Y | 2.48 | [0.57, 9.13] | [1.03, 6.02] | | | |
| LU ADC | Honda **(37)** | 34 | Y | 8.53 | [2.3, 91.2] | [2.61, 27.63] | 5.52 | 0.89 | [1.77, 17.3] |
| | Kanashiki **(38)** | 140 | N | 4.47 | [1.53, 49.77] | [1.47, 13.67] | | | |
| | Mackintosh **(39)** | 36 | N | 8.3 | [1.8, 75.2] | [2.53, 27.44] | | | |
| LU SCC | Honda **(37)** | 11 | Y | 4.37 | [1.3, 7.37] | [2.51, 7.55] | 3.46 | 0.65 | [1.5, 7.95] |
| | Kanashiki **(38)** | 44 | N | 3.3 | [1.33, 23.73] | [1.31, 8.27] | | | |
| | Mackintosh **(39)** | 6 | N | 3.23 | [2.2, 8.5] | [2.08, 4.98] | | | |
| ME | Carlson **(40)** | 5 | Y | 3.13 | [1.67,11.23] | [1.69, 5.78] | | 0.48 | - |
| PA | Furukawa **(14)** | 9 | Y | 4.8 | [2.13, 8.5] | [3.07, 7.53] | 3.74 | 0.36 | [2.36, 5.94] |
| | Rezai **(41)** | 10 | Y | 2.99 | [1.13, 5.03] | [1.87, 4.83] | | | |
| SA | Galante **(42)** | 44 | Y | 0.24 | [0.05,4.23] | [0.06, 0.99] | 0.27 | 1.07 | [0.07, 1.06] |
| | Spratt **(43)** | 5 | Y | 0.83 | [0.7,5.83] | [0.42, 1.63] | | | |

Note: *$\omega$ = standard deviation of the associated normal distribution.

## *Collection and curation of PFS data*

*Table S1.3 Published PFS curves.*

| Cancer Type | Reference | N. pz | Cohort/ Treatment | Median PFS [month] | Median OS [month] | Overall response rate |
|---|---|---|---|---|---|---|
| CC | Casak 2022 **(45)** | 61 | Placebo | 1.4<br>[1.34, 1.85] | 7.5<br>[4.8, 11.1] | - |
| | Zhu 2021 **(46)***  | 59 | Placebo | 1.6<br>[1.46,1.86] | 7.5<br>[4.8, 11.1] | - |
| CR | Bendell 2011 **(47)** | 18 | Capecitabine | 2.53 | 7.6 | 7% |

| | | | | | | |
|---|---|---|---|---|---|---|
| | | | | [1.65, 3.26] | [5, 16.3] | |
| | Cutsem 2007 **(48)** | 232 | Best supportive care | 1.8 [1.77, 2.02] | 6.5 [na] | - |
| | Dasari 2023 **(49)** | 230 | Placebo | 1.8 [1.8, 1.93] | 4.8 [4, 5.8] | - |
| | Hecht 2017 **(50)** | 85 | FOLFIRI + Simtuzumab | 5.4 [3.4, 5.6] | 10.5 [9.2, 12.6] | 5.9% |
| GA | Bang 2015 **(51)** | 62 | Paclitaxel | 3.55 [2.35, 5.12] | 8.3 [na] | 9% |
| | Boku 2009 **(52)** | 234 | FU | 2.9 [1.7, 5.7] | 10.8 [5.7, 17.8] | 9% |
| | Ohtsu 2003 **(53)** | 70 | UFTM | 2.4 [1.3, 3.2] | 6 [4.6, 7.4] | 9% |
| | Vanhoefer 2000 **(54)** | 122 | ELF | 3.3 [2.9, 4.43] | 7.2 [6, 8.3] | 5.7% |
| HN | Burtness 2005 **(55)** | 60 | Cisplatin | 2.7 [1.9, 4.01] | 8 [6.1, 10.6] | 10% |
| | Cohen 2019 **(56)** | 248 | Standard-of-care therapy (methotrexate, docetaxel, or cetuximab) | 2.3 [1.79, 2.8] | 6.9 [5.9, 8] | 10% |
| | Ferris 2016 **(57)** | 121 | Standard-of-care therapy (methotrexate, docetaxel, or cetuximab) | 2.3 [1.9, 3.14] | 5.1 [4, 6] | 5.1% |
| LI | Cheng 2009* **(58)** | 76 | Placebo | 1.4 [1, 1.55] | 4.2 [3.75, 5.46] | - |
| | Llovet 2008 **(58)** | 303 | Placebo | 2.8 [2.7, 4.11] | 7.9 [6.8, 9.1] | - |
| | Zhu 2015 **(60)** | 282 | Placebo | 2.1 [1.6, 2.83] | 7.6 [6, 9.3] | - |
| ME | Chapman 2011 **(61)** | 274 | Dacarbazine | 1.6 [1.55, 1.77] | 64% alive after 6 months | 5% |
| | Hauschild 2012 **(62)** | 40 | Dacarbazine | 2.7 [1.51, 2.95] | na | 7% |
| | Kim 2013 **(63)** | 63 | Dacarbazine | 1.8 [1.78, 2.04] | 14% of death | 0% |
| PA | Conroy 2011 **(64)** | 171 | Gemcitabine | 3.3 [2.2, 3.83] | 6.8 [5.5, 7.6] | 9.4% |
| | Girardi 2019 **(65)** | 54 | Gemcitabine | 1.7 [0.98, 2.57] | 6.8 [2.6, 11.0] | 9.3% |
| | Kindler 2010 **(66)** | 256 | Gemcitabine | 2.9 [2.4, 4.52] | 5.9 [5.1, 6.9] | 10% |
| | Moore 2007 **(67)** | 284 | Gemcitabine | 3.6 [3.29, 4.11] | 5.91 [na] | 8% |
| SA | Gounder 2022 **(68)** | 97 | Placebo | 2.1 [1.51, 3.06] | 12.9 [8.54, 15.90] | - |
| | Kawai 2016 **(69)** | 16 | Placebo | 1.75 [0.93, 2.91] | 14.9 [6.8, na] | - |

Notes: *Kaplan Meyer curve for PFS was not available, information about time to progression (TTP) was used.

From each of the study reported in Table S1.3, the PFS curve was digitalized. Let $S(t)$ denote its value at time $t$ and $N$ the number of patients involved in the study. Thus, the 95%CI of $S(t)$ for any time $t$ was reconstructed, assuming that there were not censored data, based on the following step:

- the standard error of $S(t)$ was approximated as $SE = \sqrt{S(t)(1 - S(t))/N}$;

- the 2.5 and 97.5 percentiles were approximated respectively as:

$$L(t) = S(t)e^{\frac{z_{0.025}}{\ln(S(t))} \cdot \frac{SE}{S(t)}} \text{ and } U(t) = S(t)e^{\frac{-z_{0.025}}{\ln(S(t))} \cdot \frac{SE}{S(t)}}$$

where $z_{0.025}$ was the 2.5$^{th}$ percentile of the normal distribution.

## Supplementary Material S2: Mathematical methods

### *Calculation of time of progression*

Based on a simplified version of the RECIST (74), progressive disease (PD) events due to target lesions progression were defined as a 20% increase of the sum of longest diameters of target tumor lesions. To compute time of progression, $t_{event}$, tumors were assumed to be composed by a single spherical lesion. Let *d* be the tumor diameter. Thus, a PD event occurs in $t_{event}$ if:

$$\boldsymbol{d(t_{event}) = 1.2d_0} \qquad \text{(Eq. S2.1)}$$

where $\boldsymbol{d_0}$ is the basal tumor diameter. Using the volume of a sphere, it followed that

$$\boldsymbol{V(t_{event}) = \frac{4}{3}\pi\left(\frac{d(t_{event})}{2}\right)^3 = \frac{4}{3}\pi\left(\frac{1.2d_0}{2}\right)^3 = 1.2^3V_0 = 1.728V_0} \qquad \text{(Eq. S2.2)}$$

where $V_0 = \frac{4}{3}\boldsymbol{\pi}\left(\frac{d_0}{2}\right)^3$ was the basal tumor volume. Thus, the tumor volume change associated to a 20% increase in diameter corresponded to a 1.728-fold change. Let now suppose that tumor volume grows exponentially with a rate $\lambda$, thus:

$$\boldsymbol{V(t_{event}) = V_0 e^{\lambda t_{event}}}. \qquad \text{(Eq. S2.3)}$$

Equaling the right expressions of Eq. S2.2 and S2.3, it followed:

$$\boldsymbol{V_0 e^{\lambda t_{event}} = V_0 1.728}$$

and applying the logarithm

$$\boldsymbol{t_{event} = \frac{ln(1.728)}{\lambda}}.$$

For simplicity, in this work we assumed that tumor lesion is spherical in shape and grows accordingly. We demonstrated that, under this assumption, a disease progression event (i.e., 20% increase of longest diameter) can express as 1.728-fold increase in tumor volume. This relationship still holds also for not-spherical tumors under the hypothesis that tumor growth rate is the same in the three spatial dimensions (a condition that is intrinsically true for spherical mass).

For example, if we consider an ellipsoidal tumor (a common more realistic alternative to spherical shape assumption), its volume is given by:

$$\boldsymbol{V(t) = \frac{4}{3}\pi \cdot L(t) \cdot l_1(t) \cdot l_2(t)} \qquad \text{(Eq. S2.4)}$$

where $L(t)$ is the radius of the longest length, i.e., $\boldsymbol{L}(t) = \boldsymbol{d}(t)/2$, and $l_1(t), l_2(t)$ the radius of the shorter ones. Under the hypothesis that tumor growth follows the same dynamics in all the three spatial dimensions, also the radius of shorter lengths can express as a function of $\boldsymbol{d}(t)$, i.e., $l_1(t) = \alpha_1 L(t)$ and $l_2(t) = \alpha_2 L(t)$ with $\alpha_1$, $\alpha_2$ constants ≤ 1. Thus, it followed that the tumor volume is given by:

$$\boldsymbol{V(t)} = \left(\frac{\mathbf{4}}{\mathbf{3}}\boldsymbol{\pi}\cdot\boldsymbol{\alpha_1\alpha_2}\cdot\left(\frac{\mathbf{d(t)}}{\mathbf{2}}\right)^3\right). \qquad \text{(Eq. S2.5)}$$

Combining Eq.S2.1 and Eq.S2.5, it followed that when a progression event occurs, the tumor volume is:

$$\boldsymbol{V(t_{event})} = \left(\frac{\mathbf{4}}{\mathbf{3}}\boldsymbol{\pi}\cdot\boldsymbol{\alpha_1\alpha_2}\cdot\left(\frac{\mathbf{1.2^3}\,\boldsymbol{d_0}}{\mathbf{2}}\right)^3\right) = \mathbf{1.2^3}\boldsymbol{V_0} = \mathbf{1.728}\boldsymbol{V_0} \qquad \text{(Eq. S2.6)}$$

where $V_{\mathbf{0}} = \frac{\mathbf{4}}{\mathbf{3}}\boldsymbol{\pi} \cdot \alpha_1\alpha_2 \cdot \left(\frac{d_0}{2}\right)^{\mathbf{3}}$ **.** This is the same equation derived under the assumption that tumor is spherical.

## Supplementary Material S3: Results

### *Mathematical modeling of the tumor growth in PDX mice*

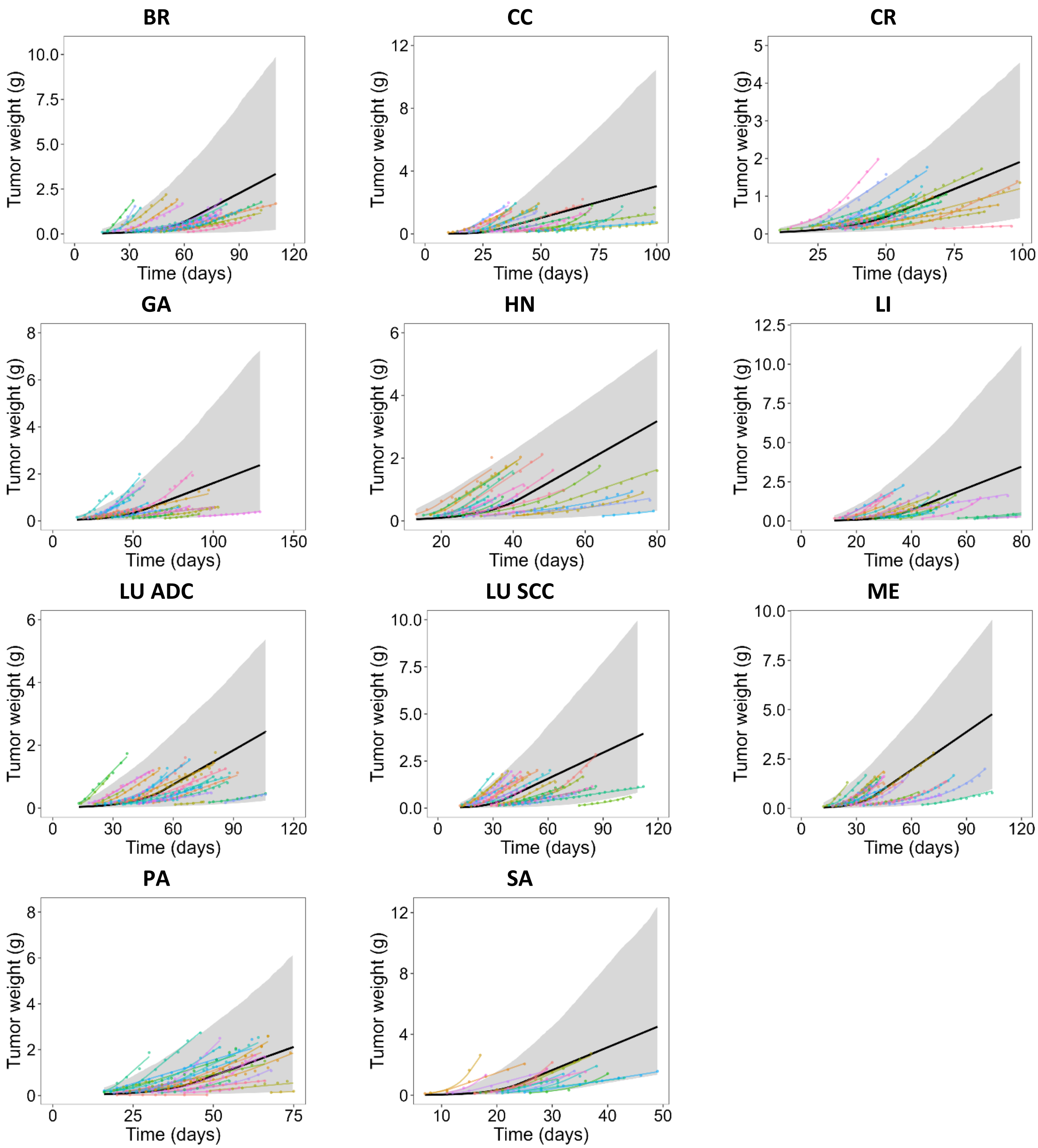


*Figure S3.1: Fitting plots of the population Simeoni growth models in PDX mice. For each cancer type, colored dots and lines represent the individual observed and predicted tumor weight profiles stratified by PDX mouse model; black line marks the typical model prediction; grey area is the 90% CI of model predictions (2500 simulations).*

*Table S3.1 - Parameter estimates of the population Simeoni tumor growth models in PDX mice together with estimation uncertainty (CV%).*

| **Cancer Type** | **$\lambda_0$ [1/day] - Rate of exponential growth** | | **$\lambda_1$ [cm$^3$/day]- Rate of linear growth** | | **$W_0$ [g]- Initial tumor weight** | | **b [-] – Coefficient of RUV model** |
|---|---|---|---|---|---|---|---|
| | **$\lambda_{0,pop}$** | **$\omega_{\lambda 0}$** | **$\lambda_{1,pop}$** | **$\omega_{\lambda 1}$** | **$W_{0,pop}$** | **$\omega_{w0}$** | |
| **BR** | 0.066 (10%) | 0.50 (15%) | 0.053 (17%) | 0.67 (18%) | 0.013 (21%) | 1.02 (14%) | 0.066 (5%) |
| **CC** | 0.142 (9%) | 0.37 (17%) | 0.040 (18%) | 0.84 (16%) | 0.003 (25%) | 0.46 (24%) | 0.117 (7%) |
| **CR** | 0.057 (8%) | 0.39 (16%) | 0.030 (14%) | 0.59 (18%) | 0.027 (14%) | 0.64 (14%) | 0.072 (5%) |
| **GA** | 0.053 (10%) | 0.5 (14%) | 0.026 (20%) | 0.79 (18%) | 0.024 (14%) | 0.69 (15%) | 0.072 (5%) |
| **HN** | 0.088 (10%) | 0.5 (15%) | 0.065 (8%) | 0.23 (25%) | 0.018 (16%) | 0.76 (15%) | 0.083 (7%) |
| **LI** | 0.110 (12%) | 0.58 (15%) | 0.069 (18%) | 0.75 (20%) | 0.009 (24%) | 1.03 (18%) | 0.088 (6%) |
| **LU ADC** | 0.064 (11%) | 0.55 (14%) | 0.037 (12%) | 0.46 (19%) | 0.017 (14%) | 0.65 (14%) | 0.061 (5%) |
| **LU SCC** | 0.100 (11%) | 0.55 (15%) | 0.046 (13%) | 0.63 (15%) | 0.012 (17%) | 0.81 (15%) | 0.063 (5%) |
| **ME** | 0.096 (10%) | 0.51 (15%) | 0.064 (13%) | 0.42 (30%) | 0.014 (16%) | 0.68 (19%) | 0.064 (8%) |
| **PA** | 0.081 (11%) | 0.54 (15%) | 0.050 (15%) | 0.67 (16%) | 0.016 (12%) | 0.54 (13%) | 0.093 (5%) |
| **SA** | 0.200 (8%) | 0.27 (21%) | 0.15 (21%) | 0.70 (23%) | 0.006 (20%) | 0.48 (24%) | 0.117 (10%) |

*Notes: Individual model parameters were supposed to be log-normally distributed: $P_i = P_{pop} exp(\eta_i)$ where $P_{pop}$ was the typical population parameter (median) and η a normally distributed random effect with mean zero and standard deviation $\boldsymbol{\omega_P}$.*

*Table S3.2 – Individual parameter estimates of the Simeoni tumor growth model in PDX mice.*

| **Cancer Type** | **PDX** | **$\lambda_0$ [1/day] Rate of exponential growth** | **$\lambda_1$ [cm$^3$/day] Rate of linear growth** | **$W_0$ [g] Initial tumor weight** |
|---|---|---|---|---|
| BR | BR10014 | 0.050 | 0.022 | 0.013 |
| | BR10539 | 0.049 | 0.025 | 0.013 |
| | BR10582 | 0.060 | 0.047 | 0.015 |
| | BR1115 | 0.075 | 0.085 | 0.065 |
| | BR1282 | 0.286 | 0.122 | 0.001 |
| | BR1283 | 0.061 | 0.049 | 0.007 |
| | BR1458 | 0.111 | 0.068 | 0.009 |
| | BR1474 | 0.049 | 0.024 | 0.024 |
| | BR2014 | 0.059 | 0.040 | 0.008 |
| | BR3267 | 0.043 | 0.034 | 0.040 |
| | BR5009 | 0.042 | 0.054 | 0.029 |
| | BR5010 | 0.040 | 0.057 | 0.027 |
| | BR5011 | 0.040 | 0.052 | 0.060 |
| | BR5013 | 0.049 | 0.106 | 0.037 |
| | BR5015 | 0.136 | 0.133 | 0.012 |
| | BR6695 | 0.057 | 0.053 | 0.019 |
| | BR9456 | 0.078 | 0.049 | 0.030 |

| | | | | |
|---|---|---|---|---|
| | BR9464 | 0.058 | 0.059 | 0.014 |
| | BR9465 | 0.049 | 0.048 | 0.029 |
| | BR9466 | 0.061 | 0.034 | 0.011 |
| | BR9469 | 0.060 | 0.059 | 0.003 |
| | BR9479 | 0.062 | 0.071 | 0.009 |
| | BR9480 | 0.077 | 0.015 | 0.002 |
| | BR9493 | 0.061 | 0.040 | 0.008 |
| | BR9494 | 0.222 | 0.174 | 0.001 |
| CC | CC6679 | 0.135 | 0.044 | 0.004 |
| | CC6639 | 0.256 | 0.051 | 0.004 |
| | CC6638 | 0.160 | 0.065 | 0.018 |
| | CC6279 | 0.153 | 0.058 | 0.006 |
| | CC6216 | 0.158 | 0.083 | 0.003 |
| | CC0449 | 0.088 | 0.010 | 0.002 |
| | CC11307 | 0.097 | 0.018 | 0.004 |
| | CC1470 | 0.088 | 0.151 | 0.003 |
| | CC6204 | 0.118 | 0.034 | 0.003 |
| | CC6205 | 0.138 | 0.042 | 0.004 |
| | CC6600 | 0.078 | 0.132 | 0.002 |
| | CC6604 | 0.162 | 0.127 | 0.006 |
| | CC6607 | 0.083 | 0.032 | 0.002 |
| | CC6609 | 0.155 | 0.061 | 0.005 |
| | CC6614 | 0.092 | 0.011 | 0.003 |
| | CC6625 | 0.205 | 0.091 | 0.007 |
| | CC6637 | 0.166 | 0.046 | 0.004 |
| | CC6645 | 0.140 | 0.020 | 0.003 |
| | CC6658 | 0.216 | 0.091 | 0.005 |
| | CC6680 | 0.135 | 0.012 | 0.004 |
| | CC6724 | 0.095 | 0.046 | 0.004 |
| | CC9326 | 0.130 | 0.007 | 0.003 |
| | CC9506 | 0.207 | 0.072 | 0.003 |
| CR | CR0004 | 0.077 | 0.047 | 0.024 |
| | CR0012 | 0.063 | 0.019 | 0.012 |
| | CR0150 | 0.063 | 0.012 | 0.015 |
| | CR0170 | 0.036 | 0.040 | 0.086 |
| | CR0193 | 0.105 | 0.050 | 0.021 |
| | CR0196 | 0.060 | 0.033 | 0.007 |
| | CR0205 | 0.080 | 0.037 | 0.023 |
| | CR1519 | 0.079 | 0.083 | 0.060 |
| | CR1801 | 0.051 | 0.012 | 0.014 |
| | CR2110 | 0.056 | 0.017 | 0.026 |
| | CR2161 | 0.056 | 0.034 | 0.034 |
| | CR2394 | 0.080 | 0.059 | 0.007 |
| | CR2517 | 0.044 | 0.041 | 0.072 |
| | CR2518 | 0.050 | 0.025 | 0.041 |
| | CR2519 | 0.064 | 0.018 | 0.023 |

| | | | | |
|---|---|---|---|---|
| | CR2524 | 0.081 | 0.023 | 0.035 |
| | CR2814 | 0.042 | 0.032 | 0.025 |
| | CR3079 | 0.040 | 0.032 | 0.044 |
| | CR3150 | 0.065 | 0.024 | 0.014 |
| | CR3315 | 0.071 | 0.036 | 0.022 |
| | CR3496 | 0.053 | 0.066 | 0.039 |
| | CR3612 | 0.080 | 0.022 | 0.022 |
| | CR6219 | 0.053 | 0.031 | 0.037 |
| | CR6227 | 0.039 | 0.027 | 0.046 |
| | CR6228 | 0.017 | 0.028 | 0.043 |
| GA | GA0006 | 0.09 | 0.048 | 0.02 |
| | GA0023 | 0.12 | 0.069 | 0.025 |
| | GA0044 | 0.11 | 0.075 | 0.011 |
| | GA0046 | 0.082 | 0.015 | 0.012 |
| | GA0055 | 0.043 | 0.0088 | 0.02 |
| | GA0080 | 0.12 | 0.046 | 0.0095 |
| | GA0087 | 0.04 | 0.026 | 0.05 |
| | GA0095 | 0.018 | 0.026 | 0.039 |
| | GA0098 | 0.043 | 0.013 | 0.019 |
| | GA0119 | 0.045 | 0.058 | 0.044 |
| | GA0138 | 0.064 | 0.013 | 0.036 |
| | GA0151 | 0.03 | 0.026 | 0.029 |
| | GA0318 | 0.046 | 0.023 | 0.052 |
| | GA0429 | 0.11 | 0.029 | 0.014 |
| | GA2101 | 0.043 | 0.011 | 0.033 |
| | GA2278 | 0.047 | 0.017 | 0.018 |
| | GA3055 | 0.044 | 0.026 | 0.005 |
| | GA3121 | 0.11 | 0.034 | 0.0099 |
| | GA3158 | 0.037 | 0.026 | 0.06 |
| | GA3839 | 0.046 | 0.026 | 0.0097 |
| | GA6200 | 0.048 | 0.026 | 0.023 |
| | GA6212 | 0.048 | 0.02 | 0.046 |
| | GA6822 | 0.03 | 0.026 | 0.028 |
| | GA6877 | 0.051 | 0.026 | 0.054 |
| | GA6898 | 0.042 | 0.026 | 0.029 |
| HN | HN0366 | 0.17 | 0.075 | 0.011 |
| | HN0586 | 0.047 | 0.065 | 0.024 |
| | HN0696 | 0.06 | 0.039 | 0.023 |
| | HN1972 | 0.072 | 0.065 | 0.009 |
| | HN2174 | 0.061 | 0.074 | 0.036 |
| | HN2221 | 0.048 | 0.065 | 0.007 |
| | HN2574 | 0.11 | 0.07 | 0.011 |
| | HN2576 | 0.13 | 0.057 | 0.010 |
| | HN2581 | 0.15 | 0.071 | 0.02 |
| | HN2583 | 0.12 | 0.074 | 0.007 |
| | HN2586 | 0.14 | 0.082 | 0.012 |

| | | | | |
|---|---|---|---|---|
| | HN2594 | 0.05 | 0.065 | 0.07 |
| | HN2606 | 0.039 | 0.065 | 0.054 |
| | HN3504 | 0.031 | 0.065 | 0.067 |
| | HN3508 | 0.13 | 0.063 | 0.014 |
| | HN3537 | 0.15 | 0.081 | 0.016 |
| | HN3642 | 0.067 | 0.065 | 0.017 |
| | HN3674 | 0.11 | 0.066 | 0.016 |
| | HN3690 | 0.12 | 0.061 | 0.008 |
| | HN3712 | 0.1 | 0.064 | 0.026 |
| | HN3792 | 0.14 | 0.076 | 0.034 |
| | HN3796 | 0.08 | 0.065 | 0.043 |
| | HN5111 | 0.14 | 0.051 | 0.04 |
| | HN5125 | 0.14 | 0.075 | 0.011 |
| | HN5126 | 0.052 | 0.065 | 0.036 |
| LI | LI0050 | 0.15 | 0.071 | 0.008 |
| | LI0348 | 0.089 | 0.028 | 0.024 |
| | LI0612 | 0.25 | 0.065 | 0.002 |
| | LI0801 | 0.097 | 0.058 | 0.024 |
| | LI1005 | 0.1 | 0.079 | 0.013 |
| | LI1025 | 0.13 | 0.059 | 0.01 |
| | LI1035 | 0.13 | 0.054 | 0.004 |
| | LI1037 | 0.14 | 0.11 | 0.001 |
| | LI1054 | 0.084 | 0.055 | 0.014 |
| | LI1055 | 0.044 | 0.069 | 0.014 |
| | LI1058 | 0.053 | 0.066 | 0.006 |
| | LI1069 | 0.11 | 0.14 | 0.008 |
| | LI1074 | 0.1 | 0.11 | 0.04 |
| | LI1078 | 0.061 | 0.066 | 0.028 |
| | LI1081 | 0.092 | 0.074 | 0.009 |
| | LI1097 | 0.24 | 0.093 | 0.006 |
| | LI1098 | 0.16 | 0.01 | 0.019 |
| | LI6206 | 0.035 | 0.071 | 0.013 |
| | LI6280 | 0.11 | 0.084 | 0.023 |
| | LI6281 | 0.12 | 0.028 | 0.015 |
| | LI6605 | 0.03 | 0.076 | 0.026 |
| | LI6610 | 0.099 | 0.14 | 0.002 |
| | LI6611 | 0.25 | 0.076 | 0.007 |
| | LI6612 | 0.21 | 0.15 | 0.006 |
| | LI6664 | 0.12 | 0.15 | 0.036 |
| LU ADC | LU1147 | 0.064 | 0.023 | 0.007 |
| | LU11606 | 0.077 | 0.057 | 0.012 |
| | LU1235 | 0.093 | 0.042 | 0.017 |
| | LU1380 | 0.092 | 0.026 | 0.009 |
| | LU1452 | 0.033 | 0.036 | 0.014 |

| | | | | |
|---|---|---|---|---|
| | LU2038 | 0.039 | 0.027 | 0.029 |
| | LU2049 | 0.043 | 0.040 | 0.032 |
| | LU2071 | 0.053 | 0.018 | 0.025 |
| | LU2505 | 0.053 | 0.034 | 0.031 |
| | LU2535 | 0.029 | 0.036 | 0.047 |
| | LU5165 | 0.064 | 0.072 | 0.029 |
| | LU5176 | 0.076 | 0.045 | 0.016 |
| | LU5187 | 0.055 | 0.022 | 0.015 |
| | LU5194 | 0.042 | 0.032 | 0.005 |
| | LU5209 | 0.028 | 0.037 | 0.057 |
| | LU5212 | 0.090 | 0.039 | 0.032 |
| | LU5240 | 0.033 | 0.037 | 0.040 |
| | LU5245 | 0.070 | 0.050 | 0.022 |
| | LU5247 | 0.069 | 0.058 | 0.007 |
| | LU5349 | 0.145 | 0.037 | 0.009 |
| | LU5371 | 0.035 | 0.036 | 0.014 |
| | LU5381 | 0.135 | 0.032 | 0.008 |
| | LU6412 | 0.048 | 0.025 | 0.034 |
| | LU6414 | 0.183 | 0.068 | 0.012 |
| | LU6425 | 0.205 | 0.064 | 0.011 |
| LU SCC | LU0350 | 0.223 | 0.078 | 0.006 |
| | LU0357 | 0.046 | 0.073 | 0.045 |
| | LU0367 | 0.052 | 0.030 | 0.003 |
| | LU0395 | 0.082 | 0.031 | 0.010 |
| | LU0697 | 0.086 | 0.018 | 0.007 |
| | LU0741 | 0.041 | 0.014 | 0.034 |
| | LU0743 | 0.150 | 0.095 | 0.018 |
| | LU0884 | 0.074 | 0.051 | 0.019 |
| | LU1143 | 0.137 | 0.058 | 0.010 |
| | LU1155 | 0.141 | 0.019 | 0.012 |
| | LU1160 | 0.058 | 0.096 | 0.023 |
| | LU1204 | 0.190 | 0.115 | 0.015 |
| | LU1206 | 0.077 | 0.048 | 0.042 |
| | LU1423 | 0.063 | 0.030 | 0.018 |
| | LU1661 | 0.185 | 0.054 | 0.007 |
| | LU1690 | 0.222 | 0.044 | 0.009 |
| | LU1776 | 0.086 | 0.024 | 0.005 |
| | LU3075 | 0.061 | 0.023 | 0.011 |
| | LU6439 | 0.160 | 0.087 | 0.013 |
| | LU6440 | 0.123 | 0.106 | 0.022 |
| | LU6901 | 0.139 | 0.036 | 0.009 |
| | LU6905 | 0.154 | 0.048 | 0.002 |
| | LU6917 | 0.043 | 0.023 | 0.041 |
| | LU9357 | 0.136 | 0.092 | 0.010 |
| | LU9358 | 0.171 | 0.061 | 0.005 |
| ME | ME1154 | 0.085 | 0.064 | 0.022 |

| | | | | |
|---|---|---|---|---|
| | ME11971 | 0.144 | 0.089 | 0.009 |
| | ME11972 | 0.139 | 0.087 | 0.009 |
| | ME12047 | 0.260 | 0.109 | 0.004 |
| | ME12056 | 0.052 | 0.050 | 0.030 |
| | ME12057 | 0.109 | 0.082 | 0.023 |
| | ME12068 | 0.113 | 0.105 | 0.014 |
| | ME12070 | 0.048 | 0.023 | 0.008 |
| | ME12079 | 0.147 | 0.092 | 0.018 |
| | ME12080 | 0.100 | 0.053 | 0.032 |
| | ME12107 | 0.088 | 0.032 | 0.025 |
| | ME12120 | 0.050 | 0.077 | 0.027 |
| | ME12149 | 0.157 | 0.052 | 0.006 |
| | ME12172 | 0.105 | 0.055 | 0.009 |
| | ME12208 | 0.136 | 0.073 | 0.011 |
| | ME12212 | 0.090 | 0.037 | 0.030 |
| | ME12216 | 0.045 | 0.073 | 0.023 |
| | ME12217 | 0.071 | 0.104 | 0.027 |
| | ME12222 | 0.047 | 0.061 | 0.019 |
| | ME13996 | 0.155 | 0.059 | 0.007 |
| | ME2194 | 0.134 | 0.101 | 0.006 |
| | ME2319 | 0.044 | 0.065 | 0.042 |
| | ME5285 | 0.139 | 0.056 | 0.014 |
| | ME9384 | 0.149 | 0.054 | 0.008 |
| | MR12035 | 0.054 | 0.054 | 0.021 |
| PA | PA0372 | 0.011 | 0.053 | 0.019 |
| | PA0692 | 0.081 | 0.053 | 0.023 |
| | PA1194 | 0.045 | 0.054 | 0.07 |
| | PA1198 | 0.08 | 0.082 | 0.018 |
| | PA1222 | 0.038 | 0.038 | 0.01 |
| | PA1233 | 0.051 | 0.013 | 0.018 |
| | PA1265 | 0.13 | 0.034 | 0.019 |
| | PA1280 | 0.092 | 0.028 | 0.022 |
| | PA1301 | 0.095 | 0.044 | 0.034 |
| | PA1306 | 0.084 | 0.04 | 0.007 |
| | PA1332 | 0.21 | 0.12 | 0.007 |
| | PA1338 | 0.14 | 0.11 | 0.013 |
| | PA1390 | 0.09 | 0.066 | 0.02 |
| | PA2410 | 0.08 | 0.09 | 0.043 |
| | PA3013 | 0.093 | 0.055 | 0.013 |
| | PA3029 | 0.098 | 0.051 | 0.014 |
| | PA3065 | 0.12 | 0.041 | 0.027 |
| | PA3126 | 0.1 | 0.034 | 0.014 |
| | PA3127 | 0.062 | 0.064 | 0.017 |
| | PA3136 | 0.12 | 0.13 | 0.008 |
| | PA3137 | 0.095 | 0.055 | 0.008 |
| | PA3139 | 0.09 | 0.12 | 0.006 |

| | | | | |
|---|---|---|---|---|
| | PA6233 | 0.055 | 0.054 | 0.013 |
| | PA6259 | 0.098 | 0.024 | 0.02 |
| | PA6265 | 0.075 | 0.015 | 0.013 |
| SA | SA0639 | 0.295 | 0.125 | 0.014 |
| | SA10199 | 0.156 | 0.239 | 0.003 |
| | SA13127 | 0.167 | 0.081 | 0.009 |
| | SA13226 | 0.161 | 0.046 | 0.005 |
| | SA13389 | 0.160 | 0.169 | 0.006 |
| | SA3224 | 0.192 | 0.160 | 0.006 |
| | SA3283 | 0.170 | 0.142 | 0.007 |
| | SA3296 | 0.195 | 0.309 | 0.007 |
| | SA3829 | 0.189 | 0.148 | 0.007 |
| | SA3831 | 0.148 | 0.059 | 0.005 |
| | SA4062 | 0.166 | 0.217 | 0.006 |
| | SA4094 | 0.239 | 0.096 | 0.008 |
| | SA4097 | 0.306 | 0.275 | 0.006 |
| | SA4109 | 0.203 | 0.082 | 0.005 |
| | SA4128 | 0.215 | 0.269 | 0.004 |

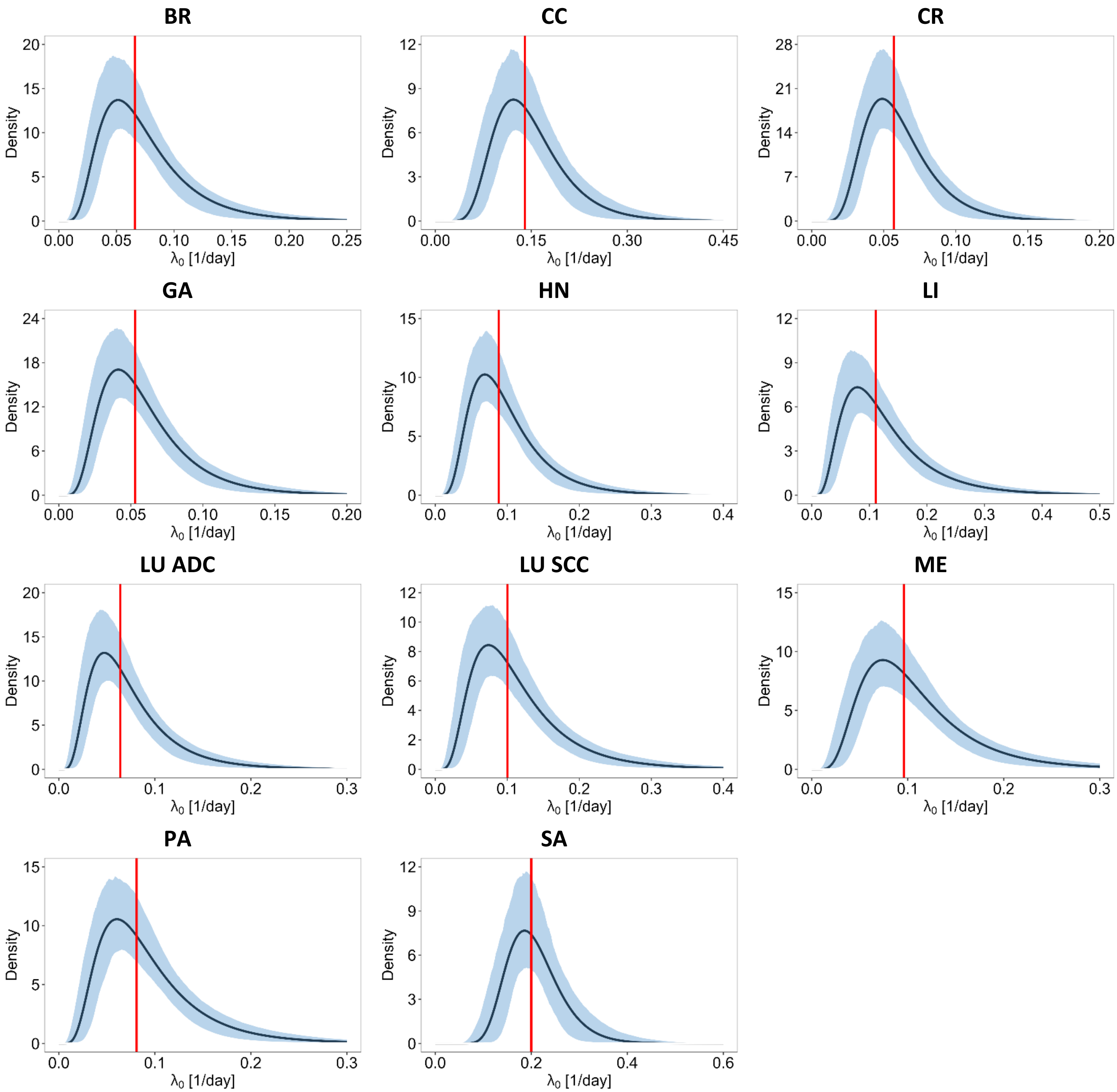


*Figure S3.2: Log-normal distributions of the parameter $\lambda_0$ of the Simeoni growth model in PDX mice. Black solid lines represent the nominal densities (corresponding to the $\boldsymbol{\lambda_{0,pop}}$ and $\boldsymbol{\omega_{\lambda_0}}$ values reported in Table S3.1). Red vertical line marks the typical (median) value. Blue bands are the 95%PIs of the densities obtained propagating uncertainty of parameter estimates (1000 values of $\boldsymbol{\lambda_{0,pop}}$ and $\boldsymbol{\omega_{\lambda_0}}$ were extracted assuming a normal distribution).*

## *Scaling of the exponential tumor growth rate from mice to human*

*Table S3.3 Scaled exponential tumor growth rate in humans,* $\lambda_{Human}$

| Cancer Type | Log-normal distribution of $\lambda_{Human}$* [1/month] | | Individual $\lambda_{Human}$ [1/month] from PDX mouse models | | | | |
|---|---|---|---|---|---|---|---|
| | $\lambda_{Human}$ (CV%)** | $\omega_{\lambda_{Human}}$ (CV%)** | | | | | |
| BR | 0.140 (10%) | 0.50 (15%) | BR10014 - 0.11 | BR10539 - 0.10 | BR10582 - 0.13 | BR1115 - 0.16 | BR1282 - 0.61 |
| | | | BR1283 - 0.13 | BR1458 - 0.24 | BR1474 - 0.1 | BR2014 - 0.13 | BR3267 - 0.09 |
| | | | BR5009 - 0.09 | BR5010 - 0.09 | BR5011 - 0.09 | BR5013 - 0.1 | BR5015 - 0.29 |
| | | | BR6695 - 0.12 | BR9456 - 0.17 | BR9464 - 0.12 | BR9465 - 0.11 | BR9466 - 0.13 |
| | | | BR9469 - 0.13 | BR9479 - 0.13 | BR9480 - 0.16 | BR9493 - 0.13 | BR9494 - 0.47 |
| CC | 0.298 (9%) | 0.37 (17%) | CC6679 -0.29 | CC6639 - 0.54 | CC6638 - 0.34 | CC6279 – 0.33 | CC6216 – 0.34 |
| | | | CC0449 - 0.19 | CC11307 - 0.21 | CC1470 - 0.19 | CC6204 - 0.25 | CC6205 - 0.29 |
| | | | CC6600 - 0.17 | CC6604 - 0.34 | CC6607 - 0.18 | CC6609 - 0.33 | CC6614 - 0.2 |
| | | | CC6625 - 0.44 | CC6637 - 0.35 | CC6645 - 0.30 | CC6658 - 0.46 | CC6680 – 0.29 |
| | | | CC6724 - 0.2 | CC9326 - 0.28 | CC9506 - 0.44 | - | - |
| CR | 0.121 (8%) | 0.39 (16%) | CR0004 – 0.16 | CR0012 – 0.13 | CR0150 – 0.13 | CR0170 – 0.0.08 | CR0193 – 0.22 |
| | | | CR0196 – 0.13 | CR0205 – 0.17 | CR1519 – 0.17 | CR1801 – 0.11 | CR2110 – 0.12 |
| | | | CR2161 – 0.12 | CR2394 – 0.17 | CR2517 – 0.09 | CR2518 – 0.11 | CR2519 – 0.14 |
| | | | CR2524 – 0.17 | CR2814 – 0.09 | CR3079 – 0.09 | CR3150 – 0.14 | CR3315 – 0.15 |
| | | | CR3496 – 0.11 | CR3612 – 0.17 | CR6219 – 0.11 | CR6227 – 0.08 | CR6228 – 0.04 |
| GA | 0.113 (10% | 0.50 (14%) | GA0006 – 0.19 | GA0023 – 0.26 | GA0044 – 0.23 | GA0046 – 0.17 | GA0055 – 0.09 |
| | | | GA0080 – 0.26 | GA0087 – 0.09 | GA0095 – 0.04 | GA0098 – 0.09 | GA0119 – 0.1 |
| | | | GA0138 – 0.14 | GA0151 – 0.06 | GA0318 – 0.1 | GA0429 – 0.23 | GA2101 – 0.09 |
| | | | GA2278 – 0.1 | GA3055 – 0.09 | GA3121 - 0.23 | GA3158 – 0.08 | GA3839 – 0.1 |
| | | | GA6200 – 0.1 | GA6212 – 0.1 | GA6822 – 0.06 | GA6877 – 0.11 | GA6898 – 0.09 |
| HN | 0.188 (10%) | 0.50 (15%) | HN0366 -0.36 | HN0586 - 0.1 | HN0696 - 0.13 | HN1972 - 0.15 | HN2174 - 0.13 |
| | | | HN2221 - 0.1 | HN2574 - 0.23 | HN2576 - 0.28 | HN2581 - 0.32 | HN2583 - 0.26 |
| | | | HN2586 - 0.3 | HN2594 - 0.11 | HN2606 - 0.08 | HN3504 - 0.07 | HN3508 - 0.28 |
| | | | HN2586 - 0.32 | HN2594 - 0.14 | HN2606 - 0.23 | HN3504 - 0.26 | HN3508 - 0.21 |
| | | | HN3792 - 0.3 | HN3796 - 0.17 | HN5111 - 0.3 | HN5125 - 0.3 | HN5126 - 0.11 |
| LI | 0.236 (12%) | 0.58 (15%) | LI0050 - 0.32 | LI0348 - 0.19 | LI0612 - 0.53 | LI0801 - 0.21 | LI1005 - 0.21 |
| | | | LI1025 - 0.28 | LI1035 - 0.28 | LI1037- 0.3 | LI1054 - 0.18 | LI1055 - 0.09 |
| | | | LI1058 - 0.11 | LI1069 - 0.23 | LI1074 - 0.21 | LI1078 - 0.13 | LI1081 - 0.2 |
| | | | LI1097 - 0.51 | LI1098 - 0.34 | LI6206 - 0.07 | LI6280 - 0.23 | LI6281 - 0.26 |
| | | | LI6605 - 0.06 | LI6610 - 0.21 | LI6611 - 0.53 | LI6612 - 0.45 | LI6664 - 0.26 |
| LU ADC | 0.136 (11%) | 0.55 (14%) | LU1147 - 0.14 | LU11606 - 0.16 | LU1235 - 0.2 | LU1380 - 0.2 | LU1452 - 0.07 |
| | | | LU2038 - 0.08 | LU2049 - 0.09 | LU2071 - 0.11 | LU2505 - 0.11 | LU2535 - 0.06 |
| | | | LU5165 - 0.14 | LU5176 - 0.16 | LU5187 - 0.12 | LU5194 - 0.09 | LU5209 - 0.06 |
| | | | LU5212 - 0.19 | LU5240 - 0.07 | LU5245 - 0.15 | LU5247 - 0.15 | LU5349 – 0.31 |
| | | | LU5371 - 0.07 | LU5381 - 0.29 | LU6412 - 0.1 | LU6414 - 0.39 | LU6425 - 0.44 |
| LU SCC | 0.213 (11%) | 0.55 (15%) | LU0350 - 0.47 | LU0357-0.1 | LU0367-0.11 | LU0395-0.17 | LU0697-0.18 |
| | | | LU0741-0.09 | LU0743-0.32 | LU0884-0.16 | LU1143-0.29 | LU1155-0.3 |
| | | | LU1160-0.12 | LU1204-0.4 | LU1206-0.16 | LU1423-0.13 | LU1661-0.39 |
| | | | LU1690-0.47 | LU1776-0.18 | LU3075-0.13 | LU6439-0.34 | LU6440-0.26 |
| | | | LU6901-0.3 | LU6905-0.33 | LU6917-0.09 | LU9357-0.29 | LU9358-0.36 |
| ME | 0.211 (10%) | 0.46 (15%) | ME1154-0.18 | ME11971-0.31 | ME11972-0.3 | ME12047-0.55 | ME12056-0.11 |
| | | | ME12057-0.23 | ME12068-0.24 | ME12070-0.1 | ME12079-0.31 | ME12080-0.21 |
| | | | ME12107-0.19 | ME12120-0.11 | ME12149-0.34 | ME12172-0.22 | ME12208-0.29 |
| | | | ME12212-0.19 | ME12216-0.1 | ME12217-0.15 | ME12222-0.1 | ME13996-0.33 |
| | | | ME2194-0.29 | ME2319-0.09 | ME5285-0.29 | ME9384-0.32 | ME120350.11 |
| PA | 0.172 (11%) | 0.54 (15%) | PA0372-0.02 | PA0692-0.17 | PA1194-0.1 | PA1198-0.17 | PA1222-0.08 |
| | | | PA1233-0.11 | PA1265-0.28 | PA1280-0.2 | PA1301-0.2 | PA1306-0.18 |

| | | | | | | | |
|---|---|---|---|---|---|---|---|
| | | | PA1332-0.45 | PA1338-0.3 | PA1390-0.19 | PA2410-0.17 | PA3013-0.2 |
| | | | PA3029-0.21 | PA3065-0.26 | PA3126-0.21 | PA3127-0.13 | PA3136-0.26 |
| | | | PA3137-0.2 | PA3139-0.19 | PA6233-0.12 | PA6259-0.21 | PA6265-0.16 |
| SA | 0.426 (8%) | 0.27 (21%) | SA0639-0.63 | SA10199-0.33 | SA13127-0.36 | SA13226-0.34 | SA13389-0.34 |
| | | | SA3224-0.41 | SA3283-0.36 | SA3296-0.42 | SA3829-0.4 | SA3831-0.32 |
| | | | SA4062-0.35 | SA4094-0.51 | SA4097-0.65 | SA4109-0.43 | SA4128-0.46 |
| | | | SA4148-0.71 | | | | |

*Notes: *Exponential tumor growth rate was parametrized as* $\boldsymbol{\lambda_{Human,i}}$=$\boldsymbol{\lambda_{Human,pop}}$*exp(*$\boldsymbol{\eta_{\lambda_{Human},i}}$*) where* $\boldsymbol{\lambda_{Human,pop}} = \boldsymbol{\lambda_{0,pop}}(\boldsymbol{BW_{Human}}/\boldsymbol{BW_{Mice}})^{-\alpha}$ *was the typical value (median) and* $\boldsymbol{\eta_{\lambda_{Human}}}$ *a normally distributed variable with mean zero and standard deviation* $\boldsymbol{\omega_{\lambda_{Human}}} = \boldsymbol{\omega_{\lambda_0}}$*. **Coefficient of variations (CV%) of the* $\boldsymbol{\lambda_{Human,pop}}$ *and* $\boldsymbol{\omega_{\lambda_{Human}}}$ *parameters were obtained propagating the estimation uncertainty of the mice-related parameters (i.e.,* $\boldsymbol{\lambda_{0,pop}}$ *and* $\boldsymbol{\omega_{\lambda_0}}$*).*

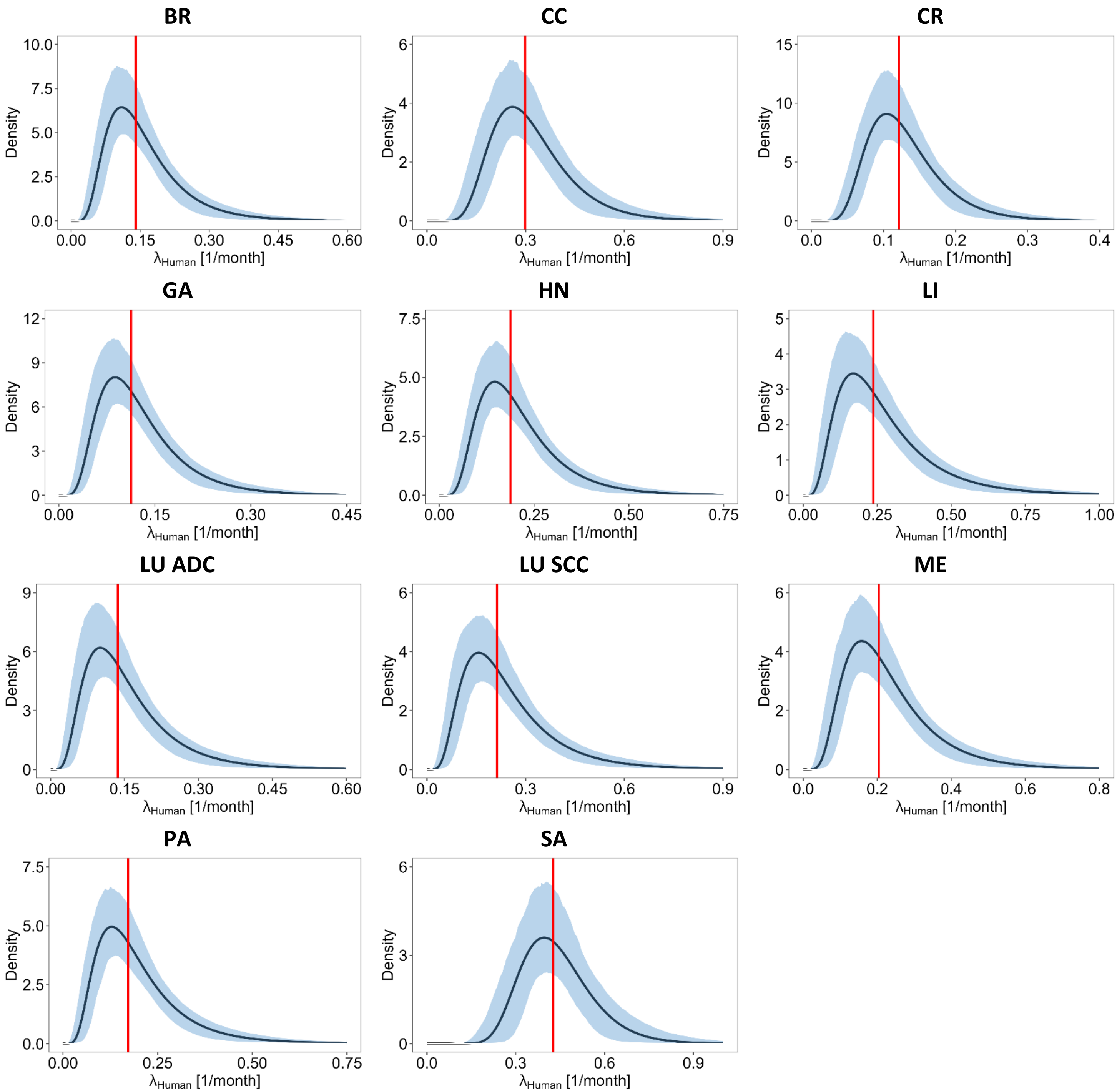


*Figure S3.3: Log-normal distributions of the exponential tumor growth rate in humans, $\lambda_{Human}$, scaled from PDX mice. Black solid lines represent the nominal densities (corresponding to the $\boldsymbol{\lambda_{Human,pop}}$ and $\boldsymbol{\omega_{\lambda_{Human}}}$ values reported in Table S3.3). Red vertical lines mark the typical (median) values. Blue bands are the 95%PIs of the densities obtained propagating estimation uncertainty of parameters (1000 values of $\boldsymbol{\lambda_{Human,pop}}$ and $\boldsymbol{\omega_{\lambda_{Human}}}$ were extracted assuming a normal distribution).*

## *Predicting the TVDT in untreated cancer patients*

For each cancer type, the 80%PI of predicted TVDTs in humans was computed following these steps:

- to account for estimation uncertainty, parameters characterizing the log-normal distribution of exponential tumor growth rate $\boldsymbol{\lambda_{Human}}$ in cancer patients, i.e., $\boldsymbol{\lambda_{Human,pop}}$ and $\boldsymbol{\omega_{\lambda_{Human}}}$, were supposed normally distributed with means equal to values reported in Table S3.3 and standard deviations derived from the corresponding CV% of estimates (see Table S3.3);
- from the normal distributions of $\boldsymbol{\lambda_{Human,pop}}$ and $\boldsymbol{\omega_{\lambda_{Human}}}$, 1000 samples, $\{\boldsymbol{\lambda_{Human,pop,i}}\}_{\boldsymbol{i=1,\ldots 1000}}$ and $\{\boldsymbol{\omega_{\lambda_{Human},i}}\}_{\boldsymbol{i=1,\ldots 1000}}$, were extracted, thus obtaining 1000 log-normal distributions of $\boldsymbol{\lambda_{Human}}$ in cancer patients, each characterized by a couple $(\boldsymbol{\lambda_{Human,pop,i}},\ \boldsymbol{\omega_{\lambda_{Human},i}})$;
- from the 1000 log-normal distributions of $\boldsymbol{\lambda_{Human}}$, the corresponding 1000 log-normal distributions of $TVDT_{Human}$ were derived, applying Eq.3;
- for each of the 1000 log-normal distributions of $TVDT_{Human}$, the 10$^{th}$ and 90$^{th}$ percentiles (*p10* and *p90*) were computed;
- the 80%PI of predicted TVDTs was defined as the 2.5$^{th}$ percentile of *p10* and 97.5$^{th}$ percentile of *p90* in order to include both the inter-patient variability and
- the parameter estimation uncertainty.

*Table S3.4 Predicted TVDTs in humans.*

| Cancer Type | Log-normal distribution of $TVDT_{Human}$ [month]* | | Individual $TVDT_{Human}$ [month] from PDX mouse models | | | | |
|---|---|---|---|---|---|---|---|
| | $TVDT_{Human}$ (CV%) | $\omega_{TVDT_{Human}}$ (CV%) | | | | | |
| BR | 4.93 (10%) | 0.50 (15%) | BR10014 – 6.46 | BR10539 – 6.6 | BR10582 – 5.41 | BR1115 – 4.32 | BR1282 – 1.14 |
| | | | BR1283 – 5.35 | BR1458 – 2.93 | BR1474 – 6.6 | BR2014 – 5.48 | BR3267 – 7.51 |
| | | | BR5009 – 7.76 | BR5010 – 8.09 | BR5011 – 8.07 | BR5013 – 6.67 | BR5015 – 2.4 |
| | | | BR6695 – 5.69 | BR9456 – 4.18 | BR9464 – 5.6 | BR9465 – 6.59 | BR9466 – 5.34 |
| | | | BR9469 – 5.41 | BR9479 – 5.23 | BR9480 - 4.23 | BR9493 – 5.36 | BR9494 – 1.47 |
| CC | 2.33 (9%) | 0.37 (17%) | CC6679 -2.41 | CC6639 - 1.27 | CC6638 - 2.04 | CC6279 - 2.13 | CC6216 - 2.06 |
| | | | CC0449 - 3.7 | CC11307 - 3.36 | CC1470 – 3.7 | CC6204 – 2.76 | CC6205 – 2.36 |
| | | | CC6600 – 4.18 | CC6604 – 2.01 | CC6607 – 3.92 | CC6609 – 2.1 | CC6614 – 3.54 |
| | | | CC6625 – 1.59 | CC6637 – 1.96 | CC6645 – 2.33 | CC6658 – 1.51 | CC6680 – 2.41 |
| | | | CC6724 – 3.43 | CC9326 – 2.51 | CC9506 – 1.57 | - | - |
| CR | 5.71 (9%) | 0.39 (16%) | CR0004 – 4.23 | CR0012 – 5.17 | CR0150 – 5.17 | CR0170 – 9.05 | CR0193 – 3.1 |
| | | | CR0196 – 5.43 | CR0205 – 4.07 | CR1519 – 4.12 | CR1801 – 6.39 | CR2110 – 5.82 |
| | | | CR2161 – 5.82 | CR2394 – 4.07 | CR2517 – 7.4 | CR2518 – 6.51 | CR2519 – 5.09 |
| | | | CR2524 – 4.02 | CR2814 – 7.75 | CR3079 – 8.14 | CR3150 – 5.01 | CR3315 – 4.59 |
| | | | CR3496 – 6.14 | CR3612 – 4.07 | CR621 – 6.14 | CR6227 – 8.35 | CR622 – 19.16 |
| GA | 6.14 (10%) | 0.50 (14%) | GA0006 - 3.62 | GA0023 - 2.71 | GA0044 - 2.96 | GA0046 - 3.97 | GA0055 - 7.57 |
| | | | GA0080 - 2.71 | GA0087 - 8.14 | GA0095 - 18.09 | GA0098 - 7.57 | GA0119 - 7.24 |
| | | | GA0138 - 5.09 | GA0151 - 10.86 | GA0318 - 7.08 | GA0429 - 2.96 | GA2101 - 7.57 |
| | | | GA2278 - 6.93 | GA3055 - 7.4 | GA3121 - 2.96 | GA3158 - 8.8 | GA3839 - 7.08 |
| | | | GA6200 - 6.78 | GA6212 - 6.78 | GA6822 - 10.86 | GA6877 - 6.39 | GA6898 - 7.75 |
| HN | 3.69 (10%) | 0.50 (15%) | HN0366 - 1.92 | HN0586 - 6.93 | HN0696 - 5.43 | HN1972 - 4.52 | HN2174 - 5.34 |
| | | | HN2221 - 6.78 | HN2574 - 2.96 | HN2576 - 2.51 | HN2581 - 2.17 | HN2583 - 2.71 |
| | | | HN2586 - 2.33 | HN2594 - 6.51 | HN2606 - 8.35 | HN3504 - 10.5 | HN3508 - 2.51 |

| | | | | | | | |
|---|---|---|---|---|---|---|---|
| | | | HN2586 - 2.17 | HN2594 - 4.86 | HN2606 - 2.96 | HN3504 - 2.71 | HN3508 - 3.26 |
| | | | HN3792 - 2.33 | HN3796 - 4.07 | HN5111 - 2.33 | HN5125 - 2.33 | HN5126 - 6.26 |
| LI | 2.93 (12%) | 0.58 (15%) | LI0050 - 2.17 | LI0348 - 3.66 | LI0612 -. 1.3 | LI0801 - 3.36 | LI1005 - 3.26 |
| | | | LI1025 - 2.51 | LI1035 - 2.51 | LI1037 - 2.33 | LI1054 - 3.88 | LI1055 - 7.4 |
| | | | LI1058 - 6.14 | LI1069 - 2.96 | LI1074 - 3.26 | LI1078 - 5.34 | LI1081 - 3.54 |
| | | | LI1097 - 1.36 | LI1098 - 2.04 | LI6206 - 9.3 | LI6280 - 2.96 | LI6281 - 2.71 |
| | | | LI6605 - 10.86 | LI6610 - 3.29 | LI6611 - 1.3 | LI6612 - 1.55 | LI6664 - 2.71 |
| LU ADC | 5.09 (12%) | 0.55 (14%) | LU1147 - 5.09 | LU11606 - 4.23 | LU1235 - 3.5 | LU1380 - 3.54 | LU1452 - 9.87 |
| | | | LU2038 - 8.35 | LU2049 - 7.57 | LU2071 - 6.14 | LU2505 - 6.14 | LU2535 - 11.23 |
| | | | LU5165 - 5.09 | LU5176 - 4.28 | LU5187 - 5.92 | LU5194 -7.75 | LU5209 - 11.63 |
| | | | LU5212 - 3.62 | LU5240 - 9.87 | LU5245 - 4.65 | LU5247 - 4.72 | LU5349 - 2.25 |
| | | | LU5371 - 9.3 | LU5381 - 2.41 | LU6412 - 6.78 | LU6414 - 1.78 | LU6425 -1.59 |
| LU SCC | 3.26 (12%) | 0.55 (15%) | LU0350-1.46 | LU0357-7.08 | LU0367-6.26 | LU0395-3.97 | LU0697-3.79 |
| | | | LU0741-7.94 | LU0743-2.17 | LU0884-4.4 | LU1143-2.38 | LU1155-2.31 |
| | | | LU1160-5.61 | LU1204-1.71 | LU1206-4.23 | LU1423-5.17 | LU1661-1.76 |
| | | | LU1690-1.47 | LU1776-3.79 | LU3075-5.34 | LU6439-2.04 | LU6440-2.65 |
| | | | LU6901-2.34 | LU6905-2.11 | LU6917-7.57 | LU9357-2.39 | LU9358-1.9 |
| ME | 3.29 (10%) | 0.46 (15%) | ME1154-3.85 | ME11971-2.26 | ME11972-2.34 | ME12047-1.25 | ME12056-6.22 |
| | | | ME12057-2.98 | ME12068-2.89 | ME12070-6.85 | ME12079-2.22 | ME12080-3.26 |
| | | | ME12107-3.69 | ME12120-6.55 | ME12149-2.07 | ME12172-3.11 | ME12208-2.4 |
| | | | ME12212-3.61 | ME12216-7.25 | ME12217-4.6 | ME12222-6.87 | ME13996-2.11 |
| | | | ME2194-2.42 | ME2319-7.47 | ME5285-2.35 | ME9384-2.19 | ME12035-6.04 |
| PA | 4.02 (11.3) | 0.54 (15%) | PA0372-29.6 | PA0692-4.02 | PA1194-7.24 | PA1198-4.07 | PA1222-8.57 |
| | | | PA1233-6.39 | PA1265-2.51 | PA1280-3.54 | PA1301-3.43 | PA1306-3.88 |
| | | | PA1332-1.55 | PA1338-2.33 | PA1390-3.62 | PA2410-4.07 | PA3013-3.5 |
| | | | PA3029-3.32 | PA3065-2.71 | PA3126-3.26 | PA3127-5.25 | PA3136-2.71 |
| | | | PA3137-3.43 | PA3139-3.62 | PA6233-5.92 | PA6259-3.32 | PA6265-4.34 |
| SA | 1.63 (8%) | 0.27 (21%) | SA0639-1.1 | SA10199-2.09 | SA13127-1.95 | SA13226-2.02 | SA13389-2.04 |
| | | | SA3224-1.7 | SA3283-1.92 | SA3296-1.67 | SA3829-1.72 | SA3831-2.2 |
| | | | SA4062-1.96 | SA4094-1.36 | SA4097-1.06 | SA4109-1.6 | SA4128-1.51 |
| | | | SA4148-0.98 | | | | |

*Notes: *Distribution of TVDT was parametrized as $TVDT$=$\boldsymbol{TVDT_{Human,pop}}$exp($\boldsymbol{\eta_{TVDT_{Human},i}}$) where $\boldsymbol{TVDT_{Human,pop}}$ was the typical value (median) and $\boldsymbol{\eta_{TVDT_{Human}}}$ a normally distributed variable with mean zero and standard deviation $\omega_{\boldsymbol{TVDT_{Human}}} = \omega_{\lambda_0}$.**Coefficient of variations (CV%) of the $\boldsymbol{TVDT_{Human,pop}}$ and $\omega_{\boldsymbol{TVDT_{Human}}}$ parameters were obtained propagating the estimation uncertainty of the mice-related parameters (i.e., $\boldsymbol{\lambda_{0,pop}}$and $\boldsymbol{\omega_{\lambda_0}}$).*

*Table S3.5 Percentage of TVDT predictions in fold-error ranges of observations*

| **Fold-error** | **% of predicted TVDT medians within fold-range of observations** | **Cancer types outside the fold-error range** |
|---|---|---|
| 1.5-fold | 91% | SA |
| 1.33-fold | 82% | SA, GA |
| 1.25-fold | 82% | SA, GA |
| 1.2-fold | 73% | SA, GA, HN |
| 1.1-fold | 64% | SA, GA, HN, BR |

*Table S3.6 Estimates of the allometric scaling exponents $\boldsymbol{\alpha}$*

| Cancer type | α estimate | SE |
|---|---|---|
| All the 11 cancer types | 0.3446 | 0.0074 |
| BR | 0.3506 | - |
| CC | 0.3335 | - |
| CR | 0.3420 | - |
| GA | 0.3753 | - |
| HN | 0.3068 | - |
| LI | 0.3451 | - |
| LU ADC | 0.3436 | - |
| LU SCC | 0.3410 | - |
| ME | 0.3232 | - |
| PA | 0.3242 | - |
| SA | 0.1070 | - |

## *Predicting the PFS curves in untreated cancer patients*

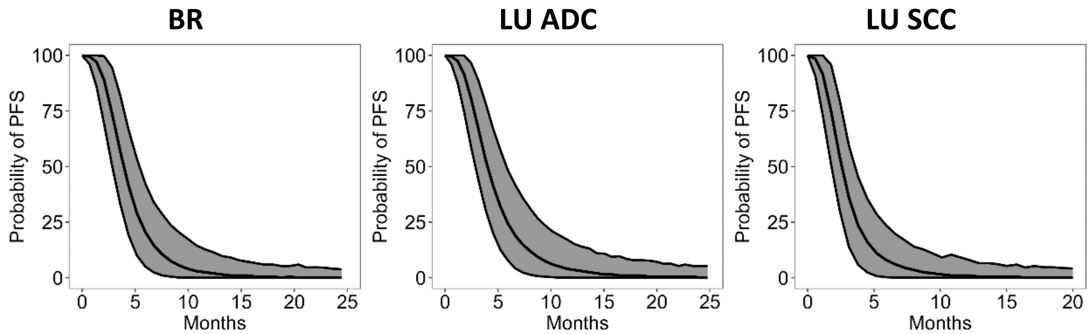


*Figure S3.5: KM-VPC plots (grey areas) generated from 1000 simulated clinical studies composed of 200 individuals, each stratified by cancer types. Median and 95% PI were reported.*

*Table S3.7. Predicted median PFS [month] in untreated cancer patients.*

| Cancer type | Predicted median PFS [month] with 95%PI |
|---|---|
| BR | 4 [3., 5.6] |
| LU ADC | 4.1 [3, 6.1] |
| LU SCC | 2.7 [2, 3.8] |